SEDGEO-105749; No of Pages 12

Sedimentary Geology 407 (2020) 105749

Contents lists available at ScienceDirect

Sedimentary Geology

journal homepage: www.elsevier.com/locate/sedgeo

Sedimentary zonation shift of tidal flats in a meso-tidal estuary

Wen Wei [a], Zhijun Dai [a,b,*], Wenhong Pang [a], Jie Wang [a], Shu Gao [a]

[a] State Key Laboratory of Estuarine & Coastal Research, East China Normal University, Shanghai 200062, China
[b] Laboratory for Marine Geology, Qingdao National Laboratory for Marine Science and Technology, Qingdao 266061, China

ARTICLE INFO

Article history:
Received 20 May 2020
Received in revised form 11 August 2020
Accepted 12 August 2020
Available online 17 August 2020

Editor: Dr. Jasper Knight

Keywords:
Zonation shift
Grain size
Sediment
Tidal flat
Changjiang Estuary

ABSTRACT

Understanding the spatial-temporal pattern of sedimentary dynamics on tidal flats is important for examining their ecological function and evolutionary trend. In this study, the dynamic state of sediments across an open-coast tidal flat of the meso-tidal Changjiang Estuary, China, on a monthly scale from December 2014 to June 2016 was examined, based on a high-spatial-resolution sedimentological-topographic survey and a collection of related meteorological-hydrological data. The results revealed a continuously distinct zonation of sediments, which transformed seaward from sand-dominance to silt dominance over a short distance. A zoning, to divide the tidal flat into a sand zone, a mixture zone and a silt zone, was delimited based on the cluster analysis of grain size frequency distributions. The zonation was highly dynamic, with the mixture zone migrating upward during summer and experiencing an uplift of 1 m in its lower boundary over the time period examined. Within each zone, the medium size and sorting coefficient of sediments tended to be smaller in winter than those in summer. Alterations of the mean tidal level likely controlled the zonation shift and sediment variations. A higher mean tidal level indicated a landward shift of the location exhibiting shear stress maxima and the mixture zone had to migrate upward to maintain an appropriate stress for the development of mixed sediments. The impacts of waves were masked under normal conditions, but during storms strong waves dominated an embedded downward displacement of the mixture zone. Characteristics of sediments covering a large region of the tidal flat changed along with zonation shifts, resulting from altered proportions among sandy, mixed and silty sediments. The study highlights that sedimentary zonation shift, under the impacts of seasonal variations in tidal level, can be a major manifestation of tidal flat sedimentary dynamics.

1. Introduction

The nature of surface sediments on tidal flats is a key factor regulating their organic sorption, pollutant accumulation and significance in global biogeochemical cycling (Costanza et al., 2014; Martinez-Garcia et al., 2015). Additionally, sediment grain size and its distribution hold important implications for sediment transport and erosion/deposition on tidal flats (Gao and Collins, 1994). Knowledge regarding the spatial-temporal pattern of sedimentary dynamics is essential to advance our understanding of the ecological function and evolutionary trend of tidal flats. This is increasingly urgent in the face of climate change and artificial interference, which have resulted in worldwide tidal flat degradation and recession (Kirwan and Megonigal, 2013).

The character of tidal flat sediments rests with the couplings between sediment source, regional hydrodynamics, and biological activity (e.g., Dyer, 1986; Friedrichs et al., 2008; Shynu et al., 2017), and thus can suffer dramatic changes in response to alterations in these processes. For tidal flats neighboring or within estuaries, the composition and quantity of riverine sediments generally play a significant role in sediment variations (e.g., Gratiot and Anthony, 2016). For example, on the Ouse Estuary, England, tidal flats were found to exhibit silty-clayey substrates in winter but sandy surface-sediments in summer, regulated by riverine sediment discharge (Uncles et al., 1998). Some studies have focused on responses of tidal flat sediments to hydrodynamics (e.g., Allen and Duffy, 1998; Alcántara-Carrió et al., 2018). For example, Allen and Duffy (1998) found that the sediments on the tidal flats of the Severn Estuary, UK, grew sandier from spring to autumn, mainly attributable to winter storminess; Shynu et al. (2017) revealed a cyclic formation and disruption of fluid muds induced by seasonally changed waves for the tidal flats of the Alleppey, India; Alcántara-Carrió et al. (2018) pointed out that the alternation of the Subtropical South Atlantic High contributed to the variations in the tidal flat sediments of the Araçá Bay, Brazil. The biological activity of tidal flats, including bioturbation, bio-adhesion, and bio-aggregation, can be independent of sediment supply or hydrodynamics and locally alters sediment texture by changing bed erodibility (Friedrichs et al., 2008). As shown in Andersen et al.'s (2005) study in the Rømø Bight, Denmark, algal biofilms, developed seasonally, led to an increase in erosion threshold and a fining of bed

* Corresponding author at: State Key Laboratory of Estuarine & Coastal Research, East China Normal University, Shanghai 200062, China.
E-mail address: zjdai@sklec.ecnu.edu.cn (Z. Dai).

https://doi.org/10.1016/j.sedgeo.2020.105749
0037-0738/

sediments. Sediment grain size variations also show relevance to tidal flat deposition/erosion, with a tendency of sediment fining as deposition occurs (Eisma, 1998), while the actual interactive-mode between sediment grain size and bed elevation was diverse among seasons (Yang et al., 2008). Additionally, sea level eustasy has been reported to bring changes to the long-term morpho-sedimentary dynamics of tidal flats (e.g., van der Wegen et al., 2017), while how seasonal fluctuations can impact the sediments have been rarely mentioned.

Tidal flat sediments are characterized by specific cross-shore distributions (e.g., Dyer, 1986; Fan, 2012). Along a transverse section, the grain size trends of sediments were found to be related to the relative dominance of tides or waves (Eisma, 1998). For example, on the extensive tidal flats in the northern Jiangsu Province, China, in a tide-dominated regime, sediments were discovered to gradually coarsen seaward (Li et al., 2005). As for the strongly wave-exposure tidal flat in the southwestern coast of South Korea, a seaward fining trend, similar to that on beaches, was detected (Yang et al., 2005). An exception was a tidal flat along the coast of Suriname, which showed the finest deposits (dominated by silty clay) and little trend variations (Lefebvre et al., 2004). Additionally, the sediments generally exhibit some transverse differentiation, with large transitions in sediment texture and grain size in some locations (e.g., Eisma, 1998; Chun, 2007). A sedimentary zonation of tidal flats has been put forward (e.g., Fan, 2012), but is less commonly used than the topographic zonation based on specific waterlines (e.g., mean high water level and mean low water level) due to its limitation in global standardization. Accordingly, variations in the spatial patterns of tidal flat sediments, especially possible sedimentary zonation shifts, have been examined in only a few studies (e.g., Chun, 2007; Alcántara-Carrió et al., 2018), which were mostly conducted in a descriptive way. While there are many studies looking at changes in beach sediments, less work has been done to variations in tidal flat sediments with sedimentary zonation shifts.

In this study, the dynamic state of sediments across an open-coast tidal flat in the Changjiang Estuary, China, was examined on a monthly scale, based on an integrated survey of cross-shore sediments and topography and a collection of meteorological and hydrological data. Major objectives of this study were to: (1) explore the spatial pattern alterations of the sediments in terms of zonation shifts; (2) detect the monthly changes in sediment grain size of different zones; and (3) analyze responses of the zonation shifts and grain size variations to external dynamics and internal topographic changes. This would give light to studies on sedimentary dynamics of tidal flats coping with similar regimes.

2. Study area

The Changjiang River is the largest river in the Eurasian Continent (Fig. 1A), exhibiting a length of 6300 km, with a multi-year average water discharge of 905×10^9 m^3/yr and a sediment discharge of 0.43 $\times 10^9$ t/yr between 1950 and 2000 (Dai et al., 2014). Nearly 47% of the riverine sediment has accumulated in the subaerial delta and estuarine system, favoring the development of tidal flats (Liu et al., 2006). The Nanhui Shoal, located in the south flank of the Changjiang Estuary, has undergone the fastest accretion with its −5 m isobaths migrating seaward at a rate of 0.5–1.2 km/yr over the past 100 years, and it is now the largest marginal shoal of the estuary (Chen, 2007). Over recent decades, the Changjiang riverine sediment discharge has decreased by 70%, largely attributable to the operation of the Three Gorges Dam. However, the shoal kept a fast accretion concentrated in the regions above −2 m as a result of large-scale siltation promotion projects, with its intertidal area significantly decayed owing to reclamation which now covers an area of 202 km^2 (Wei et al., 2019).

The field survey was conducted on an exposed tidal flat at the southern edge of the Nanhui Shoal (Fig. 1B). The tides here are semidiurnal and high mesotidal, exhibiting an average tidal range of 4.0 m during springs and a bi-direction tidal current with the principal axis parallel to the coastline (Yun, 1983). The tides have a smaller flood period and a longer duration of high water. The tidal levels can be modulated by the riverine water discharge and show significant seasonal variations, with the monthly-average tidal height in summer 0.3 m higher than that in winter (Wang et al., 2018). The winds, affected by monsoons, are southeasterly in summer and westerly in winter, with an annual-average wind speed of 4 m/s (Yun, 1983). Accordingly, the waves are generally landward in summer and offshore in winter. The multi-year average and maximum wave heights, recorded at the −5 m isobaths off the Nanhui Spit, are 1.0 m and 6.2 m, respectively (Group of Shanghai Coastal Investigation GSCI, 1988). Tropical cyclones frequently impact the region in summer (Chen, 2007). This includes typhoon Chan-hom, which is the strongest typhoon to pass within 160 km of Shanghai in the past 35 years and has made landfall roughly 140 km southeast of Shanghai on July 11th 2015 with a wind speed exceeding 40 m/s (CMR, 2015).

The intertidal region of the studied tidal flat, which was destroyed by reclamation, has developed since 2008. Around the study site, bed sediments are mainly composed of sand or silt in the intertidal region and are generally silt-dominant in the subtidal region (Yan et al., 2011). Our previous field survey in December 2011 (data published in Lin et al., 2014) and December 2014 shows that subsurface sediments (2–10 cm below the surface) in both subtidal and intertidal regions exhibit similar compositions to those of surface sediments (topmost 2 cm). The suspended sediments in the Changjiang outflow, which are transported southward along the China's coast (Liu et al., 2006), could likely impact this site, while these suspended sediments are very fine, mainly containing silt and clay and exhibiting an average medium size of 0.10 mm during 2003–2010, monitored at Datong (Gao et al., 2015). The sediment sampling section (Fig. 1C) shows a concave-up profile, with a mean gradient of ~7‰ and a low tide width of ~500 m. Elevation along the section is generally below MHWS (mean high water during springs), indicating a missing supratidal zone. Along this section, the subtidal flat of the Nanhui Shoal is quite narrow relative to that in the inner estuary and exhibits a slope of ~4‰, based on a bathymetric survey in 2013 (Dai et al., 2018).

There are several engineering interventions related to the study site. At the transect distance of 37.5–50 m is located a jetty, which weakens the waves passing by and restricts landward flows, further favoring occasional development of a small gully (Wang et al., 2018); the construction of cross-shore groins and along-shore dykes upstream of Nanhui Spit retains sediment there and would reduce fluvial suspended sediment export through the South Passage (Dai et al., 2018); and the construction of the Donghai Bridge could weaken ebb currents towards the study site. Additionally, biological activity here is not significant, given the low biomass from benthos, with no obvious evidence of diatom biofilm or sediment-mediated biological disturbance (Zhu et al., 2014).

Based on the above descriptions, the study site herein is more like a tidal flat of a concave-up profile in Friedrichs's (2011) summary, in terms of tidal flat shape and independent forcings such as relatively strong wave actions and human disturbance. However, this studied flat experiences a relatively large tidal range, large external sediment input but of unmatched composition, limited bioturbation, and faster rising tide with longer duration of high water.

3. Materials and methods

3.1. Data acquisition

3.1.1. Sediment observations

A monthly sedimentological survey was carried out over the period December 2014–June 2016. This includes an additional survey on July 15th 2015, i.e. four days after the passage of typhoon Chan-hom, to examine the impacts of this storm. During the survey, bed sediments of the topmost 2 cm were sampled every 12.5 m along the repeat fixed section (Fig. 1C). This sediment thickness corresponds to the active layer, sediments within which could represent timely responses

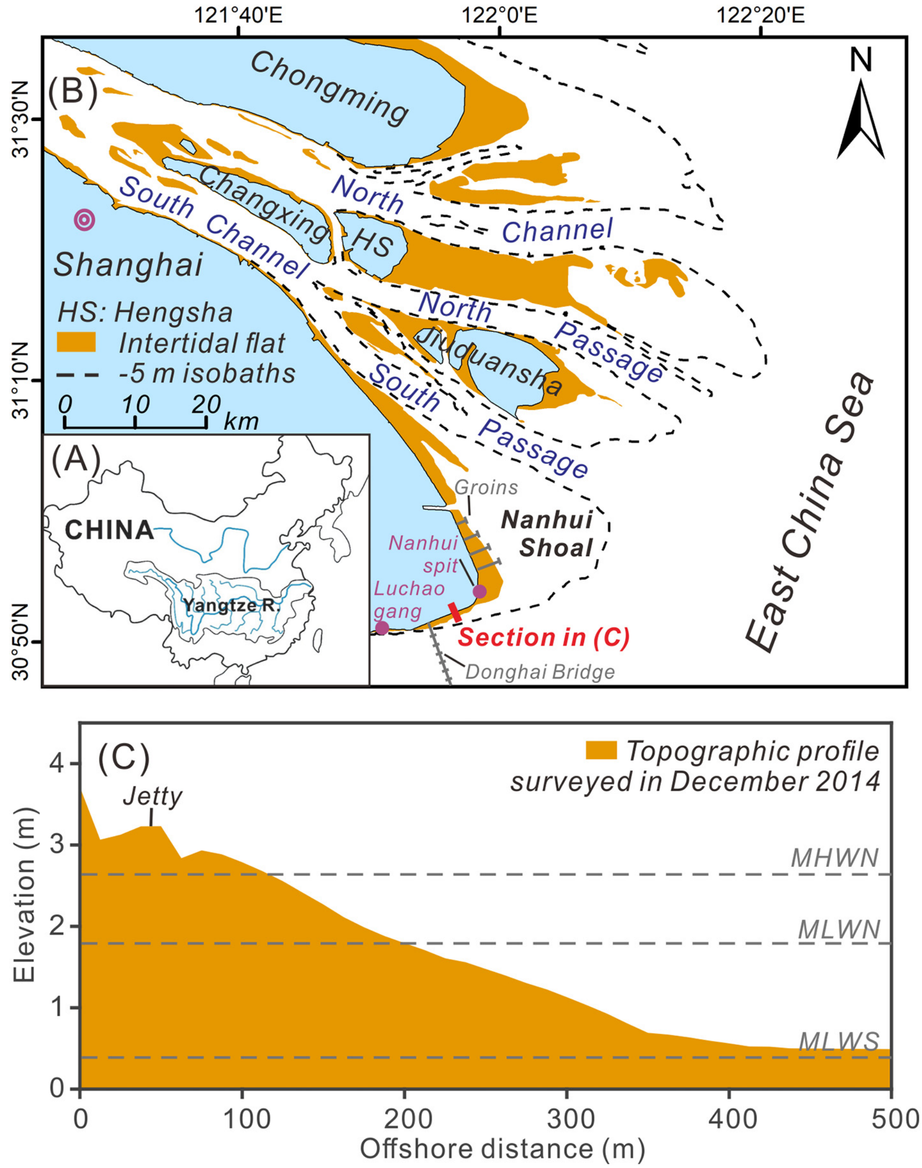

Fig. 1. Diagrams showing (A) locations of the Changjiang catchment; (B) locations of the study area; and (C) the topography of the section to conduct sedimentological-topographic survey.

to hydrodynamics (Abuodha, 2003; Kaczmarek et al., 2004). The selection of topmost 2 cm is relatively conservative, given that the intratidal erosion under moderate weather could exceed 2 cm (Zhu et al., 2014) and the erosion during two tidal cycles could exceed 15 cm under energetic conditions (Fan, 2012) around the study site. Although the survey was generally conducted during springs, the sample number varied, attributable to the variations in actual tidal elevation (Table 1). A total of 396 sediment samples have been acquired and then grain size (a series of grain fractions and mass percentage, i.e., frequency distribution of grain size) was measured by a Coulter LS 100Q grain size analyzer (Coulter, USA).

3.1.2. Topography observations

Along with the sedimentological survey, bed elevation along the section was monitored (Table 1) by a Trimble R8 GPS (Allen et al., 2012) over the period July 2015-Feburary 2016 and by a 3D terrestrial laser scanner (RIEGL-VZ4000; Riegl, 2015) at other times. These data went through a uniform georeferencing (to the 'Shanghai City coordinate' and 'Wusong Datum') and calibration (showing a vertical error within 0.02 m) and were used to analyze the linkage between topographic changes and sedimentary dynamics.

3.1.3. Meteorological and hydrological data collection

The meteorological and hydrological data were collected to examine factors impacting tidal flat sedimentary dynamics. Data on daily wind speed, significant wave height and mean wave direction were collected from a dataset named 'ERA5 hourly data on single levels from 1979 to present' in the European Centre for Medium-Range Weather Forecasts (https://www.ecmwf.int/). This is a reanalysis of global climate, with a horizontal resolution of 0.25° × 0.25° for atmospheric data and a resolution of 0.5° × 0.5° for ocean wave data. Data at the cell of (121.75°E, 31°N) was selected to represent wind and incident wave conditions around the study site. Data on monthly tidal level at Luchaogang (Fig. 1B) were collected from the Shanghai Water Authority (http://www.shanghaiwater.gov.cn/). Data on monthly Changjiang water/sediment discharge were collected from the Bulletin of China River Sediment (www.cjh.com.cn/).

3.2. Analytical methods

3.2.1. Data processing

Data on frequency distribution of grain size provided the most detailed information on sediment grains and therefore were used to define

Table 1
Overview of the monthly sedimentological and topographic survey.

No.	Date	Wind speed (m/s)	Wind direction (°)	Wave height (m)	Sample quantity	Topographic survey
1	Dec. 15th, 2014	6.4	197.9	1.7	41	Lidar
2	Jan. 22nd, 2015	5.4	160.3	2.4	38	Lidar
3	Feb. 3rd, 2015	3.7	191.1	1.6	36	Lidar
4	Mar. 1st, 2015	3.6	165.8	2.6	14	Lidar
5	Apr. 2nd,2015	8.1	350.6	2.0	21	Lidar
6	May 5th, 2015	5.1	317.7	3.5	17	Lidar
7	June 4th, 2015	3.1	320.4	4.4	20	Lidar
8	July 3rd, 2015	4.3	280.3	2.2	13	RTK
9	July 15th, 2015	4.4	284.2	2.2	31	RTK
10	Aug. 17th, 2015	4.1	236.3	1.7	15	RTK
11	Sep. 12th, 2015	6.3	148.9	4.0	25	RTK
12	Oct. 13th, 2015	1.2	226.8	2.4	25	RTK
13	Dec. 15th, 2015	5.3	160.8	1.9	25	RTK
14	Feb. 21st, 2015	6.2	300.7	2.4	25	RTK
15	Apr. 22nd, 2015	4.2	319.1	3.0	25	Lidar
16	June 21st, 2015	3.4	324.3	5.5	25	Lidar

sedimentary zonation, with the analytical method described in Section 3.2.2. Parameters including sand/silt/clay content, medium size (D_{50}), sorting coefficient (σ), skewness and kurtosis were computed following AGU (AGU, 1947) and McManus (1988), with their mean values within specific regions (divided based on the defined zonation) calculated to examine monthly variations in sediment grain size. The topographic data were used to define the elevation range (upper and lower boundaries) of the zones and then quantify the vertical displacements of these zones. Furthermore, mean/maximum significant wave heights within 1, 3 and 7 days before each survey were calculated from the original wave data. These processed wave data, together with the collected daily wind data, monthly tidal level data and monthly water/sediment discharge data, were used to distinguish factors dominating possible sedimentary zonation shifts and sediment grain size variations of the studied tidal flat, through linear regression analysis (e.g., Berry and Lindgreen, 1990).

3.2.2. Clustering analysis

The K-means clustering analysis, of high efficiency and simplicity in data classification (Han and Kamber, 2006), was introduced to delimit the sedimentary zonation. Firstly, the dataset $X_{m\times n}$ (data on grain size frequency distribution of a sample aligned in a row; m is sample quantity and n is the number of grades) was randomly assigned to k (a predetermined number) clusters, generating an initial clustering $C\{Ci, i = 1, 2, \ldots, k\}$ surrounding a center of μ_i. Then an iterative process began to minimize the following object function (J):

$$J(C_k) = \sum_{x_i \in C_k} (x_i - \mu_k)^2 \tag{1}$$

where x_i was the i^{th} sample. With sediments of each month zoned, the zonation shift could be quantified.

3.2.3. Empirical orthogonal function

The empirical orthogonal function (EOF), which could decompose a complex dataset into a small number set of uncorrelated variables (Dai et al., 2010; Wei et al., 2017), was introduced to examine the major patterns of monthly cross-shore sedimentary dynamics. Specifically, the data to be analyzed was organized in a form of $D(O)_{m\times n}$, with data for a month aligned in a single column. The EOF analysis was described as:

$$D = \sum_{i=1}^{n} t_i \times s_i \tag{2}$$

where t_i and s_i were the i^{th} eigenweighting and eigenvector, representing the temporal and spatial patterns involved in the sediment grain size changes, respectively. The first few modes, with cumulative contribution rate exceeding 75%, were adequate to examine the main information of the dataset (Dai et al., 2010).

4. Results

4.1. Cross-shore distribution of sediments

The sediments exhibited three types of grain size frequency distribution (Fig. 2), including a unimodal mode with peak frequency at 2.5–3.0 φ in the land side, a bimodal or unimodal mode exhibiting moderate frequency over grains of 2.5–5.0 φ in middle, and a unimodal mode with a peak at 4.5–5.0 φ on the seaward side. Meanwhile, the sediments were found to transform seaward from sand-dominance (of a sand content >80%) to silt-dominance (of a silt content >65%) over a short distance (dozens of meters), with D_{50} increasing abruptly from 2.7 φ to 4.6 φ (Fig. 3A, B, D; Table 2). Significant correlation ($p < .01$) was detected among the similarly distributed sand/silt content and D_{50}.

Clay content was generally small (<10%), as of either seaward increasing (e.g., during April–October 2015) or transversely uniform (e.g., during February–June 2016). σ, skewness and kurtosis showed similar distribution mode (Fig. 3E–G) and were significantly correlated ($p < .01$). They all decreased seaward gradually except in January 2015, when their values showed overall seaward increasing trends and were much smaller (>1) than other periods within the transect distance of 0–175 m. At site 2, at an offshore distance of 12.5 m, sediments of abnormally bimodal frequency distribution curve and different composition and grain size relative to the neighboring sites were found between March–July 2015 (Fig. 2D–H and Fig. 3A–G). Additionally, bed elevation increased within the distance of 0–37.5 m but decreased at 75–150 m (Fig. 3H).

4.2. Shift in sedimentary zonation

Between 2014 and 2016, sites exhibiting bimodal sediments varied (Fig. 2) and shifted frequently within a transect distance of 50–187.5 m (Fig. 3A, B, D). Given the unique cross-shore distribution of high similarity in texture in the land/sea side and dramatic changes in middle, the k was set as a value of 3 in the clustering analysis to divide the tidal flat into a sand zone, mixture zone and silt zone seaward (Fig. 4A, B). Notably, a correction was needed for site 2, where bimodal sediments with different grain sizes relative to neighboring sites were occasionally developed (Fig. 2).

Fig. 4C shows horizontal displacement of the mixture zone, based on multiple clustering analyses. Between 2014 and 2016, this zone experienced a net landward retreat of 62.5 m, with a strong tendency of

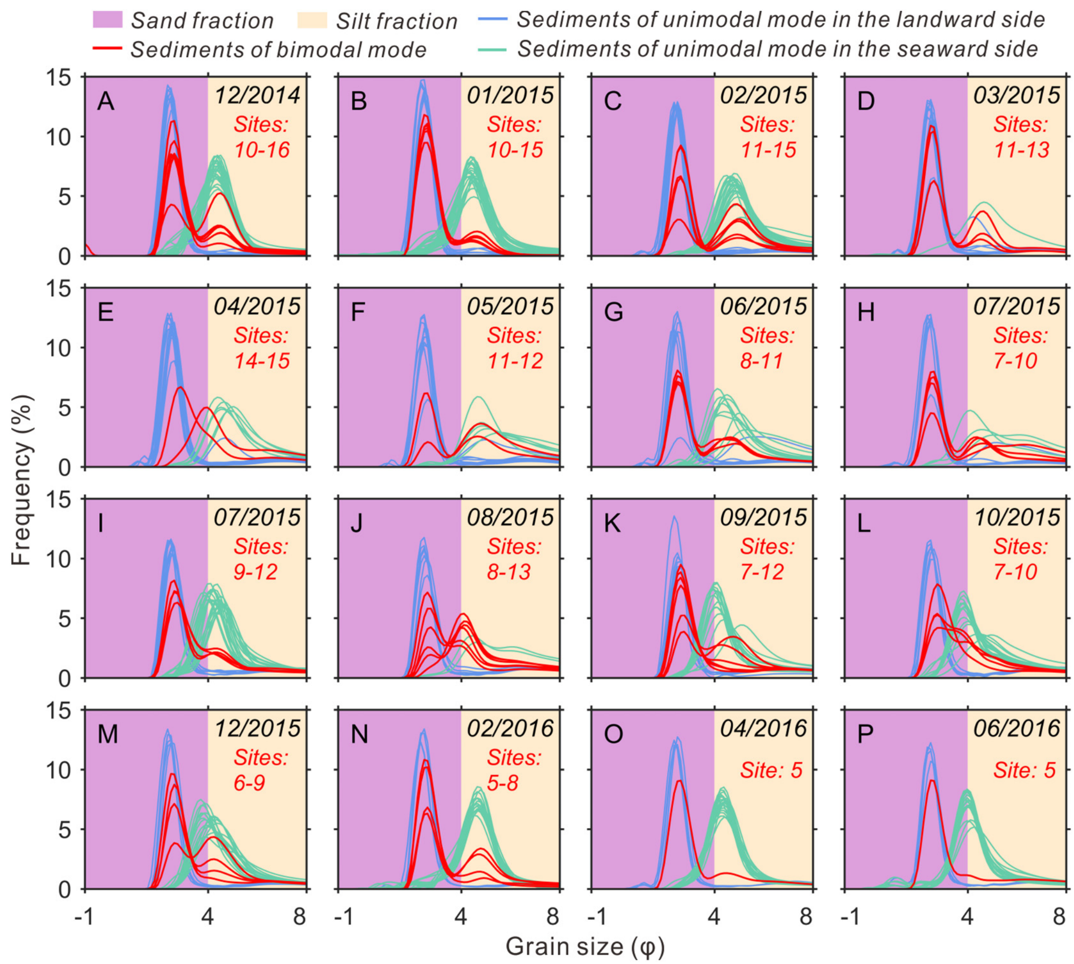

Fig. 2. Variations in grain size frequency distribution. The red line labels sediments of mixture zone, which is extracted by the K-means clustering analysis and generally shows bimodal frequency distribution. Panels (H) and (I) represents situations before and after the storm, respectively. (For interpretation of the references to colour in this figure legend, the reader is referred to the web version of this article.)

retreat in summer and embedded seaward advance between March–April 2015 and over the period just after the storm. Meanwhile, the width of the zone decreased by 75 m and showed a narrowing trend in spring. Additionally, the landward retreat of the mixture zone was generally consistent with its upward migration, being 0.3 m in terms of its upper boundary and 1 m in terms of its lower boundary over the survey period (Fig. 4D). The width of the elevation range to develop the mixture zone was found to change in a similar way to variations in its horizontal width.

4.3. Temporal variations in grain size

Shown in Fig. 5 are variations in sediment grain size of different zones. In the sand zone, D_{50} increased slightly (by 0.1 φ) and was relatively small in February and July (Fig. 5A); and σ, skewness and kurtosis all experienced sharp decreases around January 2015 and February 2016 and stayed stable over other periods (Fig. 5D, G, J). As for the mixture zone, D_{50} showed an approximately symmetric distribution, being small around February 2014 and June 2016 (Fig. 5B); and σ, skewness and kurtosis changed in a similar way to the sand zone (Fig. 5E, H, K). Variations in the four parameters for the silt zone were similar to those in the mixture zone, except for the overall increased skewness and kurtosis.

Variations in grain size at fixed locations (Sites 1–4: constant sand zone; Sites 5–16: regions undergoing zonation shift; Sites 17–25: constant silt zone) are also shown (Fig. 5). Variations at the sites 1–4 and 17–25 were always in accordance with the sand zone and silt zone, respectively. Relatively, D_{50} increased significantly by 1.3 φ and skewness and kurtosis exhibited continuous decreases after April 2015 at sites 5–16, different from the abovementioned variations in the mixture zone (Fig. 5B, E, H, K).

4.4. EOF analysis of sedimentary dynamics

D_{50}, showing distinct changes both spatially and temporally, was selected to conduct the EOF analysis. The data for sites 1–25 were interpolated to obtain a complete matrix and went through EOF analysis directly, generating three valid eigenmodes (Fig. 6). The first eigenmode, contributing 98.0% of the total variance, showed an average state of the sedimentary dynamics. Specifically, D_{50} remained large (small) in the land (sea) side and experienced a gradual increase within the distance of 50–187.5 m (Fig. 6A2), in accordance with the spatial distribution shown in Fig. 3. This first eigenweighting was small before January 2015 and showed moderate fluctuations thereafter (Fig. 6A1), resembling an intermediate state among changes in D_{50} of different zones (Fig. 5A–C).

The second and third eigenmodes, although of low contribution rates, were the major modes to explain the shifts in the spatial distribution of D_{50} and cumulatively contributed to 75% of the residual variance (Fig. 6B, C). The second eigenweighting shows negative values after May 2015 and the eigenvector became positive offshore the distance of 187.5 m (Fig. 6B). This eigenmode explained the transfer from advance to

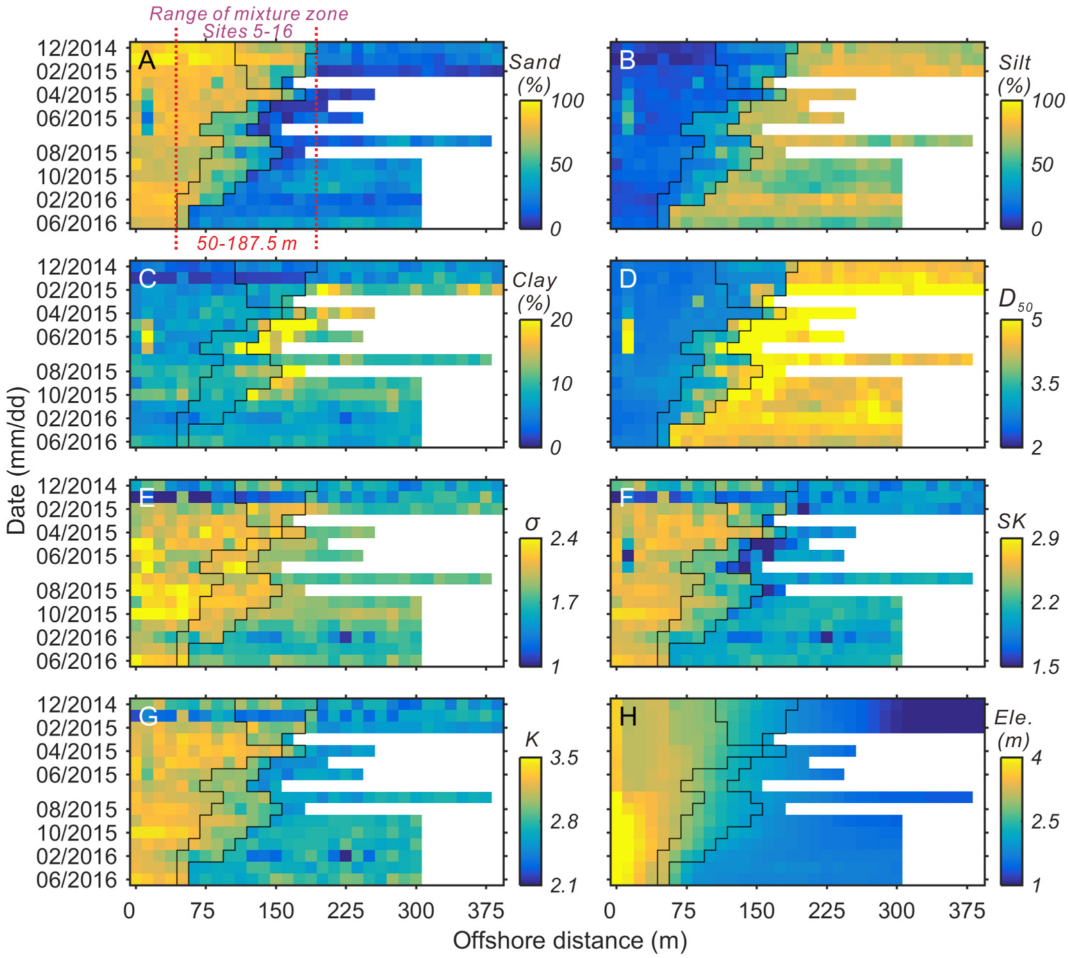

Fig. 3. Diagrams showing spatial-temporal distribution of (A) sand content, (B) silt content, (C) clay content, (D) D_{50}, (E) σ, (F) skewness and (G) kurtosis and (H) sampling elevation of the sediments. The black line labels sediments of the mixture zone, which is extracted by the clustering analysis and shows large gradients in sand/silt content and D_{50}.

Table 2
Statistics on the mean value of parameters among different zones.

Zones	Sand (%)	Silt (%)	Clay (%)	D_{50}	σ	Skewness	Kurtosis
Sand zone	80.9	12.4	6.7	2.7	2.0	2.5	3.1
Mixture zone	58.7	32.9	8.4	3.5	2.0	2.3	3.0
Silt zone	19.5	69.5	11.0	4.9	1.7	2.0	2.6

retreat for the mixture zone, beginning in May 2015. The third eigenweighting showed a pitch point in September 2015 and the eigenvector exhibited large absolute values within the distance of 50–187.5 m (Fig. 6C). Together with the second mode, this mode explained the variations in width of the mixture zone.

5. Discussion

5.1. Sedimentary zonation and its shift

Hydrodynamic sorting, relative to the character of fluvial sediments, seems to control the sediment texture and its distribution here, shown by the sandy-silty flat (Fig. 3) versus the silty-clayey Changjiang sediment input (Gao et al., 2015). This is different from the cases at the coasts of eastern England (Möller et al., 1999) and Guiana (Gratiot and Anthony, 2016). The development of sedimentary zonation under the regulation of hydrodynamic sorting could be explained by a conceptual model shown in Fig. 7. Given a wave-dominance regime manifested by the seaward fining sediments (Eisma, 1998), the transverse bed shear stress on the studied tidal flat should show a quasi-parabolic distribution (Friedrichs, 2011; Hu et al., 2015). Fine sediments are not likely to deposit on the high part of the tidal flat, where bed shear stress is enough large and a sand zone forms. In the middle of the tidal flat, bed shear stress is within an appropriate range, tending to erode just a portion of silty sediments and further resulting in a mixture of sandy and silty sediments. The suspended silty sediments could only accumulate on the seaward side, leading to the formation of a silt zone. The large tidal range, strong wave exposure (Yun, 1983) and small flat width help maintain the differentiation of bed shear stress and its induced sorting of sediments into different zones.

The sediment grains and their spatial patterns observed here are highly dynamic (Figs. 3, 4). From a geological point of view, the detected changes in sediment composition and displacements of the mixture zone might result from erosion of surface sediments and exposure of sub-surface substrate (Dyer, 1986). However, our sediment sampling from the topmost 2 cm rules out this possibility. As Kaczmarek et al. (2004) noted, the superficial sediments “remember” the hydrodynamics shaping them and the adaptation time could be as short as a few hours. Our sampled sediments of the topmost 2 cm, although likely go beyond the definition of superficial sediments by Kaczmarek et al. (2004), are within the active layer, which could exceed 15 cm in thickness based on Fan (2012)'s observation and our surveyed topographic changes. Thus, the detected sedimentary dynamics represent timely responses to hydrodynamics, presumably of an adaption time within several days. The similar composition in sediments from the surface layer and subsurface layer (Lin et al., 2014) also supports this inference.

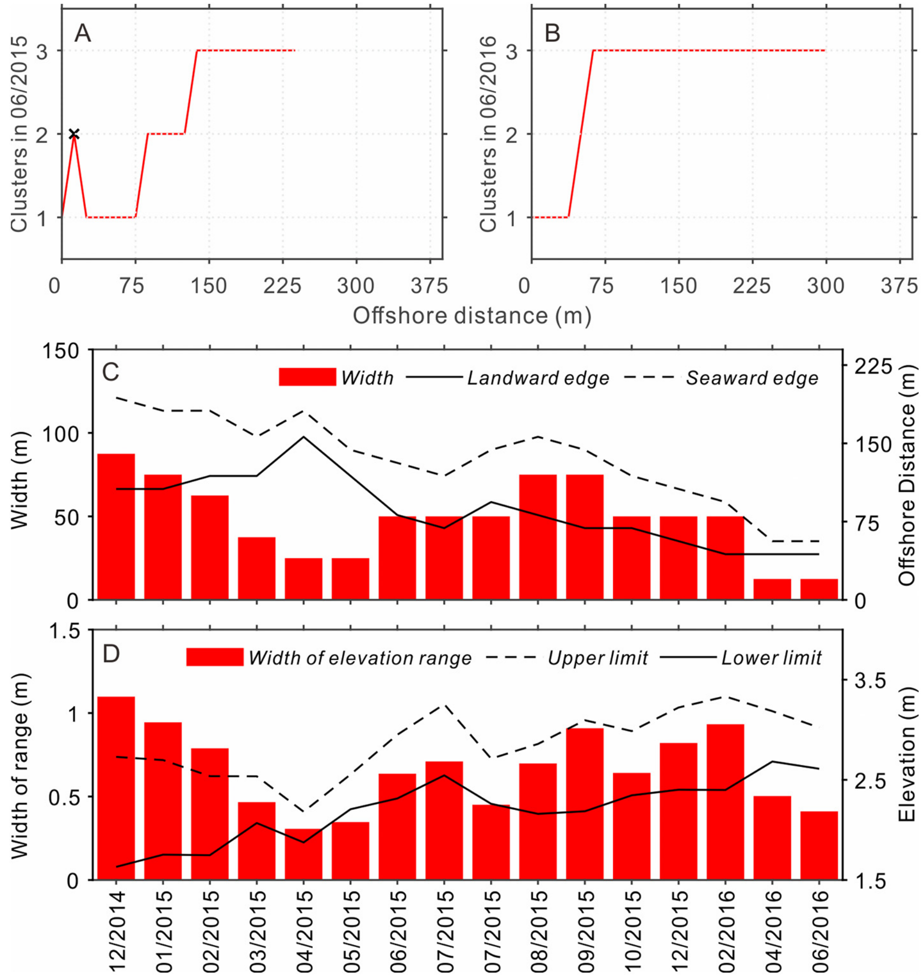

Fig. 4. (A–B) Clustering analysis results of sediments in June 2015 and June 2016, with the black cross in panel (A) labeling an incorrect classification; (C) horizontal displacement of the mixture zone; and (D) vertical displacement of the mixture zone.

Sedimentary zonation shifts could be a major manifestation of cross-shore sedimentary dynamics of tidal flats and are not unique to our study site. At Gyonggi Bay, Korea, the Han riverine mud input leads to an intrusion of mixed flat towards the sandy flat in summer (Chun, 2007). In the Araçá Bay, Brazil, the Subtropical South Atlantic High and migratory cold fronts are found to result in alterations in sediment distributions on tidal flats (Alcántara-Carrió et al., 2018). As for the tidal flat herein, riverine sediments have been proved to contribute little to flat sedimentation (Wei et al., 2019). Wind direction is deemed to play a role in sediment transport (Yun, 1983) and the prevailing onshore wind in summer is consistent with landward retreat and upward migration of the mixture zone (Figs. 4, 8A). Additionally, the fluvial control, scaled by riverine water discharge, is proved to be limited (Chen, 2007), and the impacts from wave direction is absent, as waves are generally onshore during each survey (Fig. 8C).

Seasonal fluctuations of mean tidal level (Fig. 8D), which are equivalent to sea-level eustasy, could be a factor triggering the observed zonation shifts. As shown by van der Wegen et al. (2017), sea-level rise likely induces a landward displacement of the location exhibiting shear stress maxima. Accordingly, the regions that suffer an appropriate stress for the development of mixed sediments should migrate upward as the mean tidal level becomes higher (Fig. 7), and the positive correlation between mean tidal level and upper/lower elevation limits of the mixture zone could be explained (Fig. 9). Based on the conceptual model (Fig. 7), stronger incident waves indicate an overall increase of bed shear stress (van Rijn, 1993) and therefore a downward migration of the mixture zone. However, the mixture zone shows a trend of upward displacement in June, when wave heights are relatively large (Figs. 4D, 8B). This indicates that the impacts of waves on sedimentary zonation shifts are probably masked by variations in mean tidal level under normal conditions.

5.2. Factors controlling grain size variations

Waves are acknowledged as an important factor regulating sediment grain size on open-coast tidal flats (Eisma, 1998). Stronger waves tend to accelerate resuspension of fine sediments and prevent their deposition on higher part of tidal flats, and can generate better sorted sediments with coarser grains (e.g., Shynu et al., 2017). However, in this study, both sediment size (in φ) and sorting coefficient are positively related to mean significant wave height within 7 days before each survey (Fig. 10A, C). Other processes, therefore, may contribute to the detected sediment changes in our study site, which suffers relatively strong tidal and wave actions.

On the high part of the studied tidal flat (Sites 1–4), where wave actions are the most significant, sediments are sand-dominant (Fig. 3). Accretion occurs between July–October 2015 together with a fining of surface sediments, and the surface sediments become finer again between February–June 2016 with minor deposition/erosion episodes (Figs. 3, 4). Presumably, the observed sediment fining over the above two periods, when mean tidal level increases gradually, is not induced by a net gain of finer sediments, but a result of weaker hydrodynamic

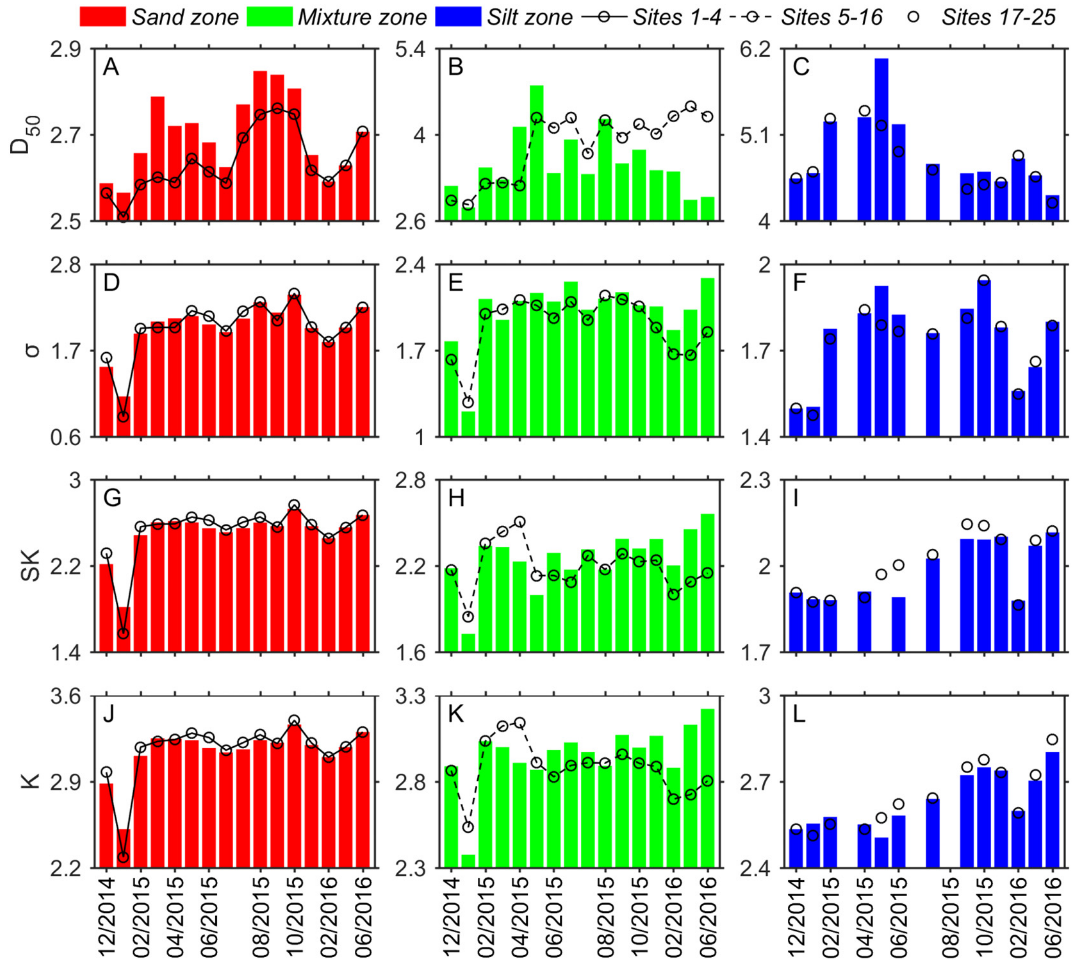

Fig. 5. Monthly variations in sediment grain size of different zones: (A–C) D_{50}, (D–F) σ, (G–I) skewness and (J–L) kurtosis. Data of site 2 is removed owing to the development of sediments obviously different from neighboring sites. The blank area in panel C, F, I and L results from deficiency of samples.

sorting. Fluctuations of mean tidal level are likely responsible for sediment variations on the high part of the flat (Fig. 10B), as wave-induced shear stress is inversely proportional to water depth (van Rijn, 1993). These modulations of seasonally-changed tidal level on hydrodynamic sorting and sediment variations have rarely been mentioned before. Additionally, the occasional development of sediments which were obviously different from the neighboring sites together with the formation of a gully at site 2 indicates that small-scale relief can also impact sediment grain size, in accordance with the findings of Williams et al. (2008) and van der Deijl et al. (2018).

In the middle of the tidal flat (Sites 5–16), variations in sediment grain size are related to sedimentary zonation shift, which is clearly shown by the last two eigenmodes of the EOF analysis (Fig. 6B, C). The upward migration of the mixture zone over the survey period indicates a smaller proportion of sandy sediments (sand zone) but an increased proportion of silty sediments (silt zone) in this region. Accordingly, sediments become finer. This is why mean tidal level, whose increase favors upward migration of the mixture zone (Fig. 9), has a statistically significant relationship with sediment grain size in this region (Fig. 10).

In the seaward part of the tidal flat (Sites 17–25), a negative correlation is found between sediment grain size and tidal level (Fig. 10B). This observed sediment coarsening along with increased mean tidal level could be explained by the model results of van der Wegen et al. (2017), as finer sediments might be transported landward owing to rising sea level. However, the changes in topographic profile indicate overall seaward sediment transport (Fig. 3H). This incomprehensible phenomenon could be attributable to the absence of data during July–August (Fig. 5) in this region.

5.3. Impacts of storms on morpho-sedimentary dynamics

Tidal flats could exhibit dramatic changes of hydrodynamics, sediment transportation and sedimentation in response to storms (e.g., Yang et al., 2003; Schuerch et al., 2014; Xie et al., 2017). In this study, erosion on the seaward side together with significant deposition on the landward side occurs just after the storm (Figs. 3H, 11A). This seemingly abnormal deposition/erosion mode relative to other periods continues over July–September 2015, indicating a duration of longer than 2 months for the storm-induced topographic changes. However, the studies of Yang et al. (2003) and Xie et al. (2017), also in the Changjiang Estuary, revealed a post-storm recovery of the tidal flats over just several days or within a month. This divergence largely results from a lack of effective sediment supply. Fast post-storm recovery can occur for sandy beaches, because sediments eroded from the upper beach are deposited on the lower beach during storms and can rapidly be redirected onshore under normal conditions (Ma et al., 2019). Yang et al.'s (2003) case in the inner estuary shows similar process, with eroded sediments from tidal flats temporarily stored within channels, also favoring a fast recovery. However, there is no large post-storm sediment surplus on the lower flat for the present study site, as the eroded sediments by storms are mainly silty and tend to be transported away as fine suspended sediment. The recovery therefore takes much longer. Further, the fine-grained Changjiang riverine sediments cannot be

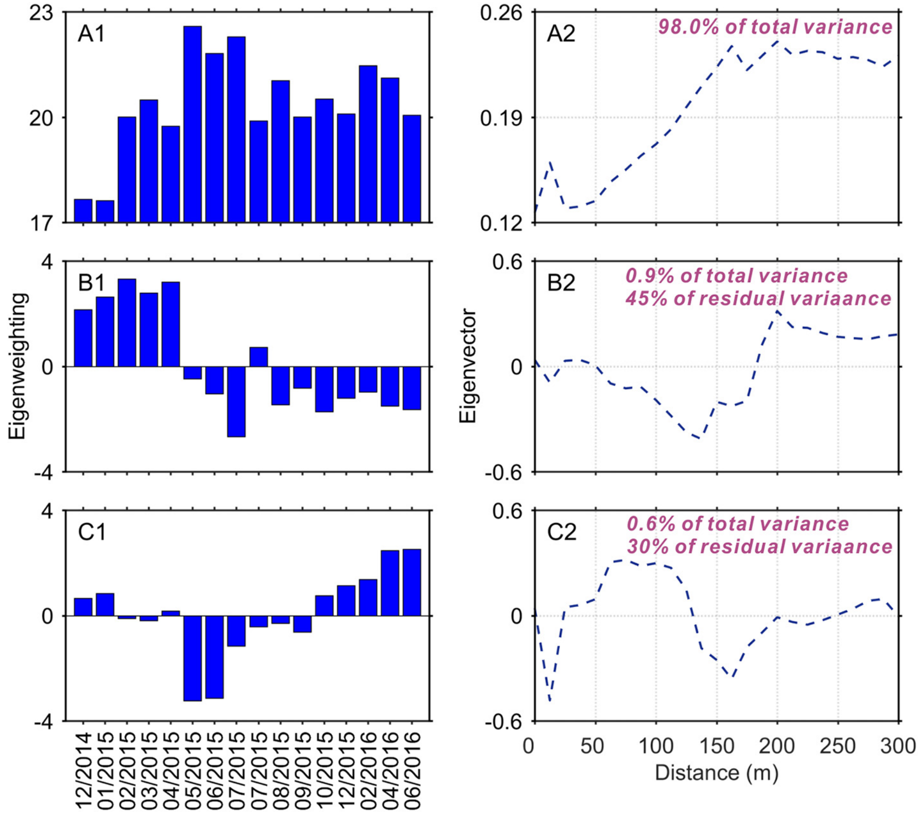

Fig. 6. EOF analysis on D_{50} of the cross-shore sediments between 2014 and 2016: (A1-2) the first eigenweighting and eigenvector; and (B1-2) and (C1-2) the second and third eigenmodes.

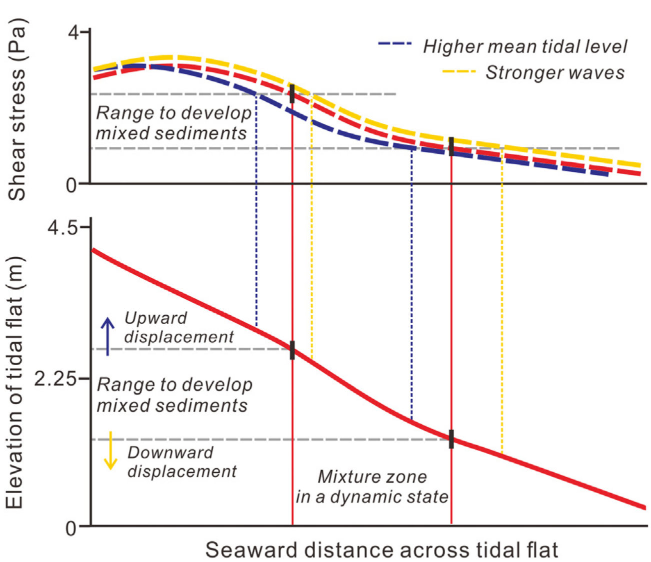

Fig. 7. Conceptual model showing the development and shift of sedimentary zonation. The upper and lower panels show bed shear stress distributions and topographic profile of a tidal flat. Notably, the bed shear stress distributions are imaginary based on analytical models of Friedrichs (2011) and Hu et al. (2015), and the order of magnitude is given based on the observations of Zhu et al. (2014) around our study site.

effective for the recovery of our studied tidal flat, that is mainly composed of sandy to silty sediments.

In terms of grain size distribution, it is found that the region of large D_{50} gradient (corresponding to the mixture zone) shows a downward migration of 0.5 m (or a seaward advance of 25 m) over July 3rd-15th 2015 and an upward migration (or landward retreat) thereafter (Fig. 11). The displacement of the mixture zone during storms could be explained by the shear stress distribution of stronger waves in the conceptual model (Fig. 7). Thus, the modulation of mean tidal level on wave-induced sorting is finite. The response of sediments likely lasts a shorter time than bathymetry. The D_{50} in the sand zone is found to be relatively large between July–September 2015, while it is not clear whether this is caused by the storm or by seasonal fluctuations of tidal level.

6. Conclusions

The monthly cross-shore sedimentary dynamics of an open-coast tidal flat in the meso-tidal Changjiang Estuary was examined, based on a suite of meteorological, hydrological, sedimentological and topographic data. Major findings included:

1) Despite the fluctuated wind/wave/tidal conditions and dramatic topographic changes, the sediments retained a zonal pattern, with sandy, mixed and silty sediments distributed seaward. The differentiation of bed shear stress, favored by strong wave-exposure, relatively large tidal range and continuously narrow flat, controlled this sedimentary zonation.
2) The mixed sediments were always located within the transect distance of 50.0–187.5 m and the mixture zone showed an upward migration during summer, with a net increase of 1 m in the lower limit of elevation range between 2014 and 2016. Seasonal fluctuations of mean tidal level contributed to the vertical displacement of the mixture zone by altering bed shear stress distributions.
3) The variations of sediment grain size on the studied tidal flat were mainly impacted by tidal level. In the high part, an increase in mean tidal level tended to induce weaken hydrodynamic sorting and further resulted in finer and more poorly sorted sediments. In the middle, sediment grain size changed along with zonation shifts, whose upward migration under increased mean tidal level led to sediment fining.

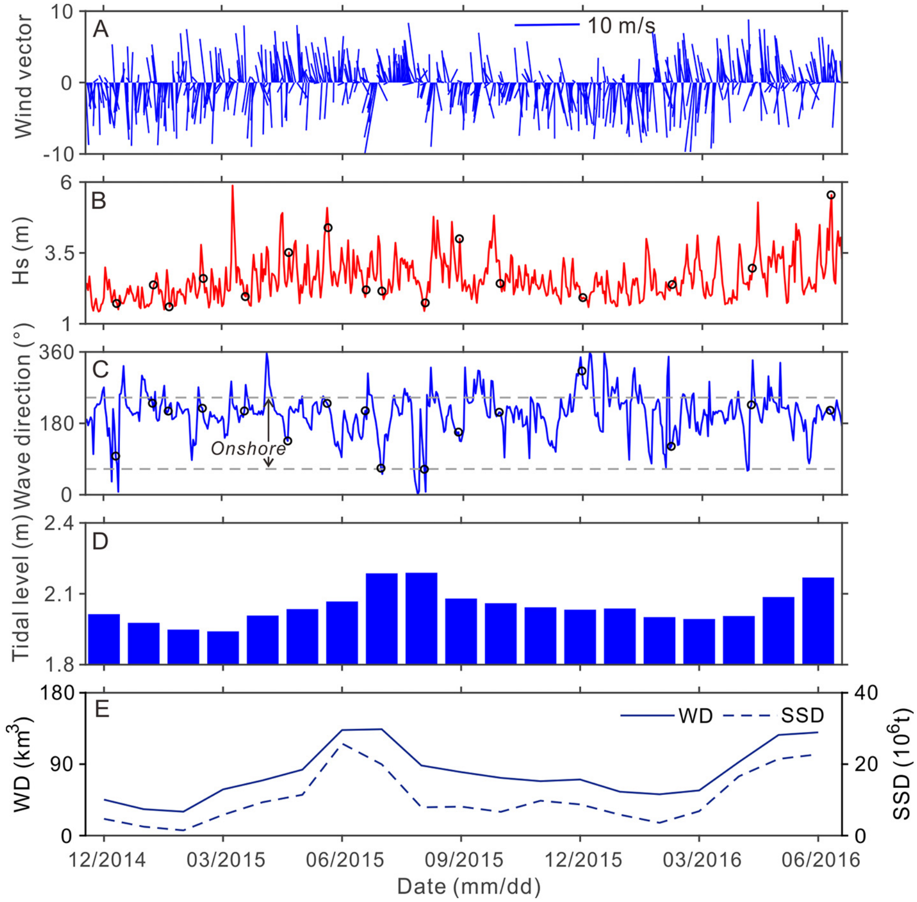

Fig. 8. Timeseries of (A) daily wind vector, (B) daily significant wave height, (C) daily wave direction, (D) monthly tidal level and (E) monthly water/sediment discharge. Each black circle in panels (B–C) corresponds to a monthly sedimentological survey.

4) The storm was responsible for the embedded downward migration of 0.5 m (or seaward advance of 25 m) of the mixture zone, and abnormal erosion on the seaward side together with significant deposition on the landward side since June 2015. The post-storm recovery of sedimentary mode takes shorter than tidal flat bathymetry, which resulted from a lack of effective sediment supply.
5) The study herein indicates that dramatic shifts in sediment zonation can be a major manifestation of sedimentary dynamics. Additionally, the seasonal fluctuations of mean tidal level, equivalent to intra-annual sea level eustasy, played the most significant role in sedimentary zonation shifts and grain size variations of tidal flats, of a mesotidal and wave-exposed regime.

Declaration of competing interest

The authors declare that they have no known competing financial interests or personal relationships that could have appeared to influence the work reported in this paper.

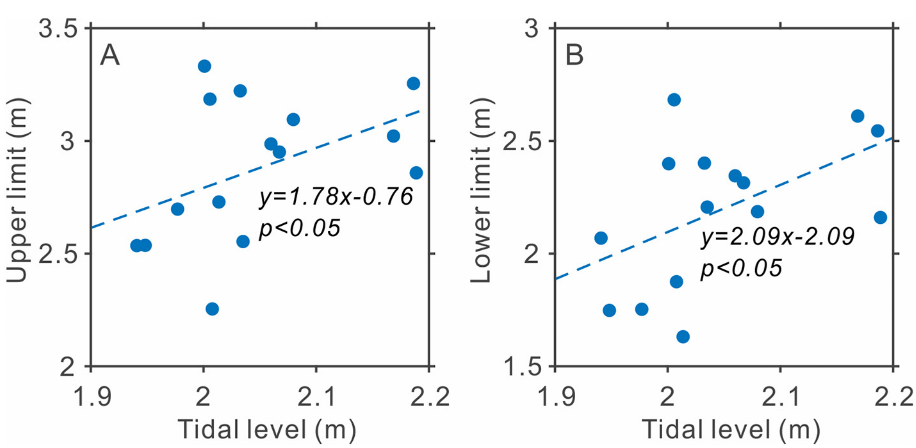

Fig. 9. Correlations between vertical displacement of the mixture zone (depicted in Fig. 4D) and hydrodynamics: (A) Upper elevation limit versus mean tidal level; and (B) lower elevation limit versus mean tidal level. Data just after the storm is removed in the analysis. Data just after the storm is removed in the analysis.

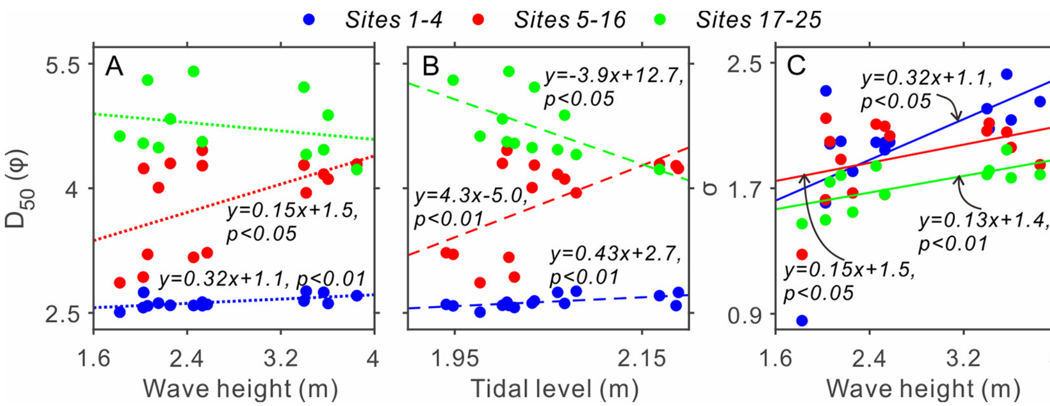

Fig. 10. D_{50} versus (A) mean significant wave height within 7 days before each survey and (B) mean tidal level; and σ versus mean significant wave height within 7 days before each survey. Data just after the storm is removed in the analysis.

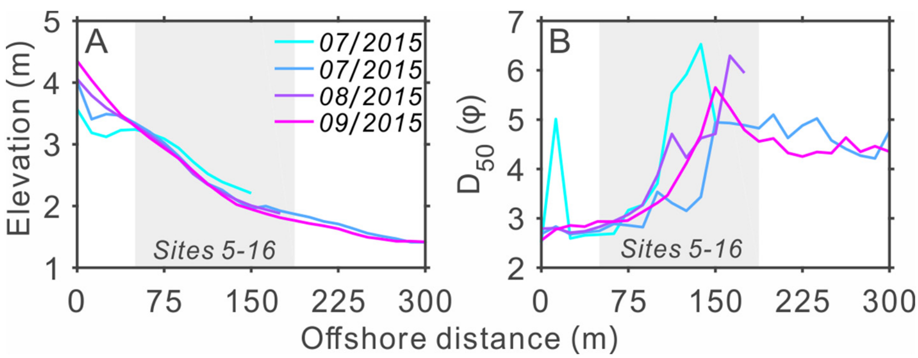

Fig. 11. Cross-shore distribution of (A) elevation and (B) D_{50}. over the period July–September 2015.

Acknowledgments

This study is supported by the Key projects of intergovernmental science and technology innovation cooperation of the Ministry of Science and Technology in China (2018YFE0109900), International Science and Technology Cooperation Project of Shanghai Science and Technology Commission (19230712400), National Natural Science Foundation of China (41806106), China Postdoctoral Science Foundation (2018M641964) and the Fundamental Research Funds for the Central Universities. We acknowledge Editor Jasper Knight and the anonymous reviewer for their comments that help to improve this paper. The data reported in this paper can be obtained by contacting the corresponding author zjdai@sklec.ecnu.edu.cn.

References

Abuodha, J.O.Z., 2003. Grain size distribution and composition of modern dune and beach sediments, Malindi Bay coast, Kenya. Journal of African Earth Sciences 36, 41–54.

AGU, 1947. Subcommittee on the sediment terminology. Report on the Subcommittee on Sediment Terminology, American Geophysical Union. Trans AGU 28, 936–938.

Alcántara-Carrió, J., Mahiques, M.M., Cazzoli y Goya, S., Fontán-Bouzas, A., 2018. Sedimentary dynamics of a subtropical tidal flat sheltered inside a coastal channel (Araçá Bay, SE Brazil). Ocean and Coastal Management 164, 32–41.

Allen, J.R.L., Duffy, M.J., 1998. Temporal and spatial depositional patterns in the Severn Estuary, SW Britain: intertidal studies at spring-neap and seasonal scales, 1991-1993. Marine Geology 146, 147–171.

Allen, T.R., Oertel, G.F., Gares, P.A., 2012. Mapping coastal morphodynamics with geospatial techniques, Cape Henry, Virginia, USA. Geomorphology 137, 138–149.

Andersen, T.J., Lund-Hansen, L.C., Pejrup, M., Jensen, K.T., Mouritsen, K.N., 2005. Biologically induced differences in erodibility and aggregation of subtidal and intertidal sediment: a possible cause for seasonal changes in sediment deposition. Journal of Marine Systems 55, 123–138.

Berry, D.A., Lindgreen, B.W., 1990. Statistics: Theory and Methods. Cole, California.

Chen, J.Y., 2007. Research and Practice of Estuary and Coast in China. Higher Education Press, Beijing (in Chinese).

China Member Report (CMR), 2015. ESCAP/WMO Typhoon Committee 10th Integrated Workshop. pp. 4–6 Retrieved January 10, 2016.

Chun, S.S., 2007. Sedimentological characteristics of southern intertidal flat of Ganghwa Island, Gyonggi Bay, western coast of Korea. US Office of Naval Research Tidal Flats DRI Planning Meeting, Honolulu, HI 5–8 June.

Costanza, R., De Groot, R., Sutton, P., Van Der Ploeg, S., Anderson, S.J., Kubiszewski, I., Farber, S., Turner, R.K., 2014. Changes in the global value of ecosystem services. Global Environmental Change 26, 152–158.

Dai, Z.J., Liu, J.T., Lei, Y.P., Zhang, X.L., 2010. Patterns of sediment transport pathways on a headland bay beach-Nanwan beach, South China: a case study. Journal of Coastal Research 26, 1096–1103.

Dai, Z.J., Liu, J.T., Wei, W., Chen, J.Y., 2014. Detection of the three Gorges Dam influence on the Changjiang (Yangtze River) submerged delta. Scientific Reports 4, 6600. https://doi.org/10.1038/srep06600.

Dai, Z.J., Fagherazzi, S., Gao, S., Mei, X.F., Ge, Z.P., Wei, W., 2018. Scaling properties of estuarine beaches. Marine Geology 404, 130–136.

Dyer, K.R., 1986. Coastal and Estuarine Sediment Dynamics. Wiley, New York.

Eisma, D., 1998. Intertidal Deposits: River Mouths, Tidal Flats, and Coastal Lagoons. CRC Press, New York.

Fan, D.D., 2012. Open-coast tidal flats. In: Davis, R.A., Dalrymple, R.W. (Eds.), Principles of Tidal Sedimentology. Springer, Dordrecht, pp. 187–229.

Friedrichs, C.T., 2011. Tidal flat morphodynamics: a synthesis. In: Hansom, J.D., Flemming, B.W. (Eds.), Treatise on Estuarine and Coastal Science: Sedimentology and Geomorphology. Elsevier, pp. 137–170.

Friedrichs, C.T., Cartwright, G.M., Dickhudt, P.J., 2008. Quantifying benthic exchange of fine sediment via continuous, non-invasive measurements of settling velocity and bed erodibility. Oceanography 21, 168–172.

Gao, S., Collins, M., 1994. Analysis of grain size trends for defining sediment transport pathways in marine environments. Journal of Coastal Research 10, 70–78.

Gao, J.H., Jia, J.J., Wang, Y.P., Yang, Y., Li, J., Bai, F., Zou, X., Gao, S., 2015. Variations in quantity, composition and grain size of Changjiang sediment discharging into the sea in response to human activities. Hydrology and Earth System Sciences 19, 645–655.

Gratiot, N., Anthony, E.J., 2016. Role of flocculation and settling processes in development of the mangrove-colonized, Amazon-influenced mud-bank coast of South America. Marine Geology 373, 1–10.

Group of Shanghai Coastal Investigation (GSCI), 1988. Report of Shanghai Coastal Comprehensive Investigation. Shanghai Scientific and Technological Press, Shanghai (in Chinese).

Han, J., Kamber, M., 2006. Data Mining, Concepts and Techniques. Morgan Kaufman Publishers, San Francisco.

Hu, Z., Wang, Z.B., Zitman, T.J., Stive, M.J.F., Bouma, T.J., 2015. Predicting long-term and short-term tidal flat morphodynamics using a dynamic equilibrium theory. Journal of Geophysical Research 120, 1803–1823.

Kaczmarek, L.M., Biegowski, J., Ostrowski, R., 2004. Modelling cross-shore intensive sand transport and changes of bed grain size distribution versus field data. Coastal Engineering 51, 501–529.

Kirwan, M.L., Megonigal, J.P., 2013. Tidal wetland stability in the face of human impacts and sea-level rise. Nature 504, 53–60.

Lefebvre, J.P., Dolique, F., Gratiot, N., 2004. Geomorphic evolution of a coastal mudflat under oceanic influences: an example from the dynamic shoreline of French Guiana. Marine Geology 209, 191–205.

Li, G.X., Yang, Z.G., Liu, Y., 2005. Studies on the Genetic Types of Sub-bottom Sedimentary Facies in the East China Seas. Chinese Science Press, Beijing (in Chinese).

Lin, Y.F., Dai, Z.J., Xie, H.L., Wei, W., Ge, Z.P., Gao, J.J., 2014. The research of exchange processes between suspended sediment near the bottom and the depositions in the Changjiang (Yangtze) Estuary. Acta Oceanologica Sinica 36, 99–110 (in Chinese with English abstract).

Liu, J.P., Li, A.C., Xu, K.H., Velozzi, D.M., Yang, Z.S., Milliman, J.D., DeMaster, D.J., 2006. Sedimentary features of the Yangtze River-derived along-shelf clinoform deposit in the East China Sea. Continental Shelf Research 26, 2141–2156.

Ma, B.B., Dai, Z.J., Pang, W.H., Ge, Z.P., Li, S.S., Mei, X.F., Huang, H., 2019. Dramatic typhoon-induced variability in the grain size characteristics of sediments at a meso-macrotidal beach. Continental Shelf Research 191, 1–9.

Martinez-Garcia, E., Carlsson, M.S., Sanchez-Jerez, P., Sánchez-Lizaso, J.L., Sanz-Lazaro, C., Holmer, M., 2015. Effect of sediment grain size and bioturbation on decomposition of organic matter from aquaculture. Biogeochemistry 125, 133–148.

McManus, J., 1988. Grain size determination and interpretation. In: Tucker, M. (Ed.), Techniques in Sedimentology. Oxford Press, Blackwell, pp. 63–85.

Möller, I., Spence, T.R., French, J.R., Leggett, D.J., Dixon, M., 1999. Wave transformation over salt marshes: a field and numerical modeling study from North Norfolk, England. Estuarine, Coastal and Shelf Science 49, 411–426.

Riegl, 2015. Riegl VZ-4000 specifications. http://www.riegl.com/uploads/tx_pxpriegldownloads/DataSheet_VZ-4000_2015-03-24.pdf. (Accessed 14 June 2015). .

Schuerch, M., Dolch, T., Reise, K., Vafeidis, A.T., 2014. Unravelling interactions between salt marsh evolution and sedimentary processes in the Wadden Sea (southeastern North Sea). Progress in Physical Geography 38, 691–715.

Shynu, R., Rao, V.P., Samiksha, S.V., Vethamony, P., Naqvi, S.W.A., Kessarkar, P.M., Babu, M.T., DineshKumar, P.K., 2017. Suspended matter and fluid mud off Alleppey, southwest coast of India. Estuarine, Coastal and Shelf Science 185, 31–43.

Uncles, R.J., Stephens, J.A., Harris, C., 1998. Seasonal variability of subtidal and intertidal sediment distributions in a muddy, macro-tidal estuary: The Humber-Ouse, UK. In: Black, K.S., Paterson, D.M., Cramp, A. (Eds.), Sedimentary Processes in the Intertidal Zone. London, Special Publications, Geological Society of London, pp. 211–220.

van der Deijl, E.C., van der Perk, M., Middelkoop, H., 2018. Establishing a sediment budget in the newly created "Kleine Noordwaard" wetland area in the Rhine-Meuse delta. Earth Surface Dynamics 6, 187–201.

van der Wegen, M., Jaffe, B.E., Amy Foxgrover, A., Roelvink, D.J.A., 2017. Mudflat morphodynamics and the impact of sea level rise in South San Francisco Bay. Estuaries and Coasts 40, 37–49.

van Rijn, L.C., 1993. Principles of Sediment Transport in Rivers, Estuaries and Coastal Seas. Aqua Publications, Amsterdam.

Wang, J., Dai, Z.J., Wei, W., Ge, Z.P., Pang, W.H., Ma, B.B., Mei, X.F., Yu, Y.W., 2018. Lidar-based recent morphodynamic study of South Nanhui tidal flat, Changjiang Estuary. Oceanologia et Limnologia Sinica 49, 756–768 (in Chinese with English abstract).

Wei, W., Dai, Z.J., Mei, X.F., Liu, J.P., Gao, S., Li, S.S., 2017. Shoal morphodynamics of the Changjiang (Yangtze) estuary: influences from river damming, estuarine hydraulic engineering and reclamation projects. Marine Geology 386, 32–43.

Wei, W., Dai, Z.J., Mei, X.F., Gao, S., Liu, J.P., 2019. Multi-decadal morpho-sedimentary dynamics of the largest Changjiang Estuarine marginal shoal: causes and implications. Land Degradation & Development 30, 2048–2063.

Williams, J.J., Carling, P.A., Amos, C.L., Thompson, C., 2008. Field investigation of ridge–runnel dynamics on an intertidal mudflat. Estuarine, Coastal and Shelf Science 79, 213–229.

Xie, W.M., He, Q., Zhang, K.Q., Guo, L.C., Wang, X.Y., Shen, J., Cui, Z., 2017. Application of terrestrial laser scanner on tidal flat morphology at a typhoon event timescale. Geomorphology 292, 47–58.

Yan, H., Dai, Z.J., Li, J.F., Zhao, J.C., Zhang, X.L., Zhao, J.K., 2011. Distributions of sediments of the tidal flats in response to dynamic actions, Yangtze (Changjiang) Estuary. Journal of Geographical Sciences 21, 719–732.

Yang, S.L., Friedrichs, C.T., Shi, Z., Ding, P.X., Zhu, J., Zhao, Q.Y., 2003. Morphological response of tidal marshes, flats and channels of the outer Yangtze River mouth to a major storm. Estuaries 26, 1416–1425.

Yang, B.C., Dalrymple, R.W., Chun, S.S., 2005. Sedimentation on a wave-dominated, open-coast tidal flat, southwestern Korea: summer tidal flat-winter shoreface. Sedimentology 53, 235–252.

Yang, S.L., Li, H., Ysebaert, T., Bouma, T.J., Zhang, W.X., Wang, Y.Y., Li, P., Li, M., Ding, P.X., 2008. Spatial and temporal variations in sediment grain size in tidal wetlands, Yangtze Delta: on the role of physical and biotic controls. Estuarine, Coastal and Shelf Science 77, 657–671.

Yun, C.X., 1983. Scouring and siltation processes of tidal flats of the Yangtze River Estuary and sediment exchange between flats and channels. Journal of Sedimentary Research 4, 43–52 (in Chinese).

Zhu, Q., Yang, S.L., Ma, Y.X., 2014. Intra-tidal sedimentary processes associated with combined wave–current action on an exposed, erosional mudflat, southeastern Yangtze River Delta, China. Marine Geology 347, 95–106.